THE JOURNAL OF BIOLOGICAL CHEMISTRY VOL. 287, NO. 20, pp. 16609–16622, May 11, 2012

Conversion of Human Steroid 5β-Reductase (AKR1D1) into 3β-Hydroxysteroid Dehydrogenase by Single Point Mutation E120H

EXAMPLE OF PERFECT ENZYME ENGINEERING[*S]

Received for publication, December 30, 2011, and in revised form, March 10, 2012 Published, JBC Papers in Press, March 20, 2012, DOI 10.1074/jbc.M111.338780

Mo Chen[‡], **Jason E. Drury**[‡], **David W. Christianson**[§], **and Trevor M. Penning**[‡1]

From the [‡]*Department of Pharmacology and Center of Excellence in Environmental Toxicology, Perelman School of Medicine, and the* [§]*Roy and Diana Vagelos Laboratories, Department of Chemistry, University of Pennsylvania, Philadelphia, Pennsylvania 19104*

Background: The aldo-keto reductase (AKR) subfamily AKR1D comprises steroid 5β-reductases, whereas the AKR1C subfamily comprises hydroxysteroid dehydrogenases.
Results: A single E120H mutation in AKR1D1 converts human steroid 5β-reductase into a 3β-hydroxysteroid dehydrogenase.
Conclusion: Glu^{120} controls the positional specificity of hydride transfer and facilitates double bond reduction.
Significance: This is an example of a perfect change-of-function that can be achieved by a single point mutation.

Human aldo-keto reductase 1D1 (AKR1D1) and AKR1C enzymes are essential for bile acid biosynthesis and steroid hormone metabolism. AKR1D1 catalyzes the 5β-reduction of Δ⁴-3-ketosteroids, whereas AKR1C enzymes are hydroxysteroid dehydrogenases (HSDs). These enzymes share high sequence identity and catalyze 4-pro-(*R*)-hydride transfer from NADPH to an electrophilic carbon but differ in that one residue in the conserved AKR catalytic tetrad, His^{120} (AKR1D1 numbering), is substituted by a glutamate in AKR1D1. We find that the AKR1D1 E120H mutant abolishes 5β-reductase activity and introduces HSD activity. However, the E120H mutant unexpectedly favors dihydrosteroids with the 5α-configuration and, unlike most of the AKR1C enzymes, shows a dominant stereochemical preference to act as a 3β-HSD as opposed to a 3α-HSD. The catalytic efficiency achieved for 3β-HSD activity is higher than that observed for any AKR to date. High resolution crystal structures of the E120H mutant in complex with epiandrosterone, 5β-dihydrotestosterone, and Δ⁴-androstene-3,17-dione elucidated the structural basis for this functional change. The glutamate-histidine substitution prevents a 3-ketosteroid from penetrating the active site so that hydride transfer is directed toward the C3 carbonyl group rather than the Δ⁴-double bond and confers 3β-HSD activity on the 5β-reductase. Structures indicate that stereospecificity of HSD activity is achieved because the steroid flips over to present its α-face to the A-face of NADPH. This is in contrast to the AKR1C enzymes, which can invert stereochemistry when the steroid swings across the binding pocket. These studies show how a single point mutation in AKR1D1 can introduce HSD activity with unexpected configurational and stereochemical preference.

Two subfamilies of NAD(P)(H)-dependent steroid transforming aldo-keto reductase (AKR)[2] exist in humans: 5β-reductase (AKR1D1) and hydroxysteroid dehydrogenases (HSDs; also known as AKR1C1–1C4). AKR1D1 catalyzes the irreversible reduction of Δ⁴-3-ketosteroids to 5β-dihydrosteroids to introduce a 90° bend at the steroid A/B ring junction (1). This *cis*-configuration is critical for bile acids to properly emulsify dietary fats and cholesterol (2). 5β-Reduced steroid hormones may be involved in parturition (3), porphyrinogenesis (4, 5), and xenoprotection (6, 7). By contrast, AKR1C enzymes catalyze the interconversion between 3-, 17-, and 20-ketosteroids and 3α/β-, 17β-, and 20α-hydroxysteroids (Scheme 1) (8). By functioning as HSDs, AKR1C enzymes regulate the ratio of active and inactive androgens, estrogens, and progestogens that can bind to nuclear receptors in target tissues (9).

AKR1D1 and AKR1C enzymes are highly homologous enzymes, sharing over 50% sequence identity and a common $(\alpha/\beta)_8$ barrel fold (10–12). Both subfamilies of enzymes bind the steroid perpendicularly to the NAD(P)(H) cofactor in the active site so that either the steroid A or D ring faces the nicotinamide ring. During reduction, a hydride from the 4-pro-(*R*)-position on the nicotinamide ring is stereospecifically transferred to the recipient double bond/carbonyl group on the steroid substrate (13). AKR1C enzymes perform the hydride

* This work was supported, in whole or in part, by National Institutes of Health (NIH) Grants R01-DK40715 and P30-ES013508 (to T. M. P.), NIH Grant GM-056838 (to D. W. C.), and NIH, NIDDK, Grant F32DK089827 (to M. C.).
[S] This article contains supplemental Figs. S1–S7.
The atomic coordinates and structure factors (codes 3UZW, 3UZX, 3UZY, and 3UZZ) have been deposited in the Protein Data Bank, Research Collaboratory for Structural Bioinformatics, Rutgers University, New Brunswick, NJ (http://www.rcsb.org/).
[1] To whom correspondence should be addressed: Dept. of Pharmacology, Perelman School of Medicine, University of Pennsylvania, 130C John Morgan Bldg., 3620 Hamilton Walk, Philadelphia, PA 19104-6084. Tel.: 215-898-9445; Fax: 215-573-2236; E-mail: penning@upenn.edu.

[2] The abbreviations used are: AKR, aldo-keto reductase; Δ⁴-adione, Δ⁴-androstene-3,17-dione; AKR1C1 to AKR1C4, human hydroxysteroid dehydrogenases; AKR1C9, rat 3α-hydroxysteroid dehydrogenase; AKR1D1, human steroid 5β-reductase; AKR1D2, rat steroid 5β-reductase; DHT, dihydrotestosterone; epiA, epiandrosterone (3β-hydroxy-5α-androstan-17-one); HSD, hydroxysteroid dehydrogenase; 20α-OHP, 20α-hydroxyprogesterone; PDB, Protein Data Bank.

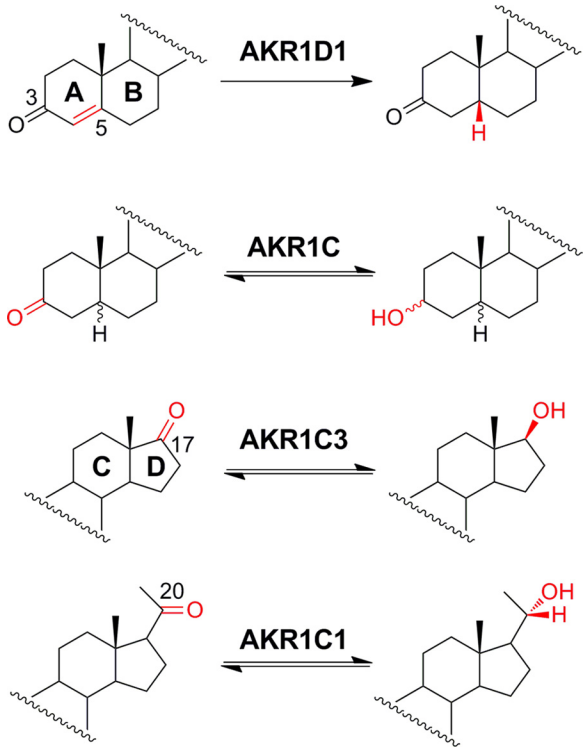

SCHEME 1. **Reactions catalyzed by AKR1D1 and human AKR1C enzymes.** Functions of the AKR1C enzymes are assigned based on their preferred substrate in the reduction of 3-/17-/20-ketosteroids. Common names and substrate preference of the AKR1C enzymes are as follows: AKR1C1 (20(3)α-HSD), 20-ketosteroid > 3-ketosteroid ~ 17-ketosteroid; AKR1C2 (3α-HSD type 3), 3-ketosteroid > 20-ketosteroid; AKR1C3 (17β-HSD type 5 or 3α-HSD type 2), 17-ketosteroid > 20-ketosteroid > 3-ketosteroid; AKR1C4 (3α-HSD type 1), 3-ketosteroid > 20-ketosteroid (8, 23).

transfer utilizing a well characterized "push-pull" mechanism (14). In the reduction direction, Tyr^{58} acts as a general acid, and His^{120} facilitates proton donation by hydrogen-bonding to Tyr^{58}. In the oxidation direction, Tyr^{58} acts as a general base assisted by Lys^{87} for proton removal, where Asp^{53} balances the positive charge on Lys^{87} through a salt bridge (Scheme 2, *left*). All residues in this report are numbered according to AKR1D1. Corresponding positions in AKR1C enzymes are Asp^{50}, Tyr^{55}, Lys^{84}, and His^{117}). These four residues are conserved across nearly all the AKR subfamilies and are collectively known as the catalytic tetrad.

The mechanism for 5β-reduction has not been fully elucidated. Even so, based on the sequence and structural similarity, it is reasonable to assume that AKR1D1 employs features of the hydride transfer mechanism displayed by the AKR1C enzymes. However, in all known 5β-reductases, one of the tetrad residues, His^{120}, is specifically substituted by a glutamate (15). Compared with ketone reduction, the 5β-reduction of a carbon-carbon double bond is much harder to achieve chemically. It requires a strong reductant and stereo-controlled hydride addition to achieve the A/B *cis* ring junction. Common chemical reductants like borohydride will reduce Δ^4-3-ketosteroids to yield the 3β-allylic alcohol, and when forced, the double bond is reduced to the 5α-configuration, but the 5β-configuration is rarely obtained (16, 17). Thus, Glu^{120} has been proposed to play a unique role in steroid 5β-reduction. According to the recently solved crystal structure of AKR1D1, the carboxylic

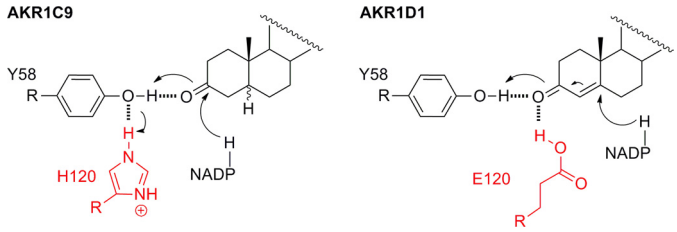

SCHEME 2. **Proposed mechanism for AKR1C enzyme-catalyzed 3-ketosteroid reduction (*left*) and AKR1D1-catalyzed 5β-reduction (*right*).**

acid group of Glu^{120} is presumed to adopt the fully protonated *anti*-oriented conformation in order to donate a hydrogen bond directly to the steroid carbonyl oxygen. This arrangement together with the general acid Tyr^{58} creates a superacidic environment that facilitates hydride transfer by activating the Δ^4-double bond and stabilizing the enolate intermediate (Scheme 2, *right*) (10).

Despite the homology between AKR1D1 and the AKR1C enzymes, no mixed activity has been observed between the two subfamilies. The glutamate-histidine substitution appears to be the key mutation that distinguishes 5β-reduction from HSD activity. To examine the role of Glu^{120} further, we introduced the E120H mutation in AKR1D1. Our kinetic characterization of the mutant demonstrates that the E120H mutation completely abolishes the 5β-reductase activity and converts AKR1D1 into a highly efficient 3β-HSD that exhibits opposite stereopreference to the majority of AKR1C enzymes, which show preference for 3α-HSD activity. Analysis of the crystal structures of the E120H mutant in complex with epiandrosterone (epiA; 3β-hydroxy-5α-androstan-17-one), 5β-dihydrotestosterone (5β-DHT), and Δ^4-androstene-3,17-dione (Δ^4-Adione) reveals that the bulky histidine imidazole ring introduced by the E120H substitution prevents penetration of the steroid into the active site so that hydride transfer is now only possible to the C3-position for ketosteroid reduction. The binding conformations of different steroid isomers also illustrate the mechanism by which HSD stereospecificity is controlled.

EXPERIMENTAL PROCEDURES

Materials—NADPH, NADH, $NADP^+$, and NAD^+ were purchased from Roche Applied Science. Steroids were purchased from Steraloids. Synthetic oligonucleotides were obtained from Invitrogen. *E. coli* strain C41 (DE3) was provided by Dr. J.E. Walker (Medical Research Council Laboratory of Molecular Biology, Cambridge, UK). The QuikChange II site-directed mutagenesis kit was purchased from Stratagene. DEAE-Sepharose Fast Flow resin and HisTrap Fast Flow column (5 ml) were purchased from GE Healthcare. [4-^{14}C]Testosterone (50 mCi/mmol), [4-^{14}C]Δ^4-androstene-3,17-dione (48 mCi/mmol), [4-^{14}C]17β-estradiol (53 mCi/mmol), [1,2,4,5,6,7-^{3}H]5α-dihydrotestosterone (5α-DHT) (110 Ci/mmol), and [9,11-^{3}H]androsterone (54 Ci/mmol) were purchased from PerkinElmer Life Sciences. [4-^{14}C]Progesterone (55 mCi/mmol) was purchased from American Radiolabeled Chemicals. All other reagents were of American Chemical Society quality or higher.

Mutagenesis, Expression, and Purification of Recombinant AKR1D1 E120H Mutant—The expression plasmid for the AKR1D1 E120H mutant was made using the pET28a-AKR1D1 construct (10) as a template by conducting site-directed mutagenesis using the QuikChange method (Stratagene) following the manufacturer's protocol. The forward primer was 5′-dGGA TCT TTA CAT CAT TCA CGT ACC AAT GGC CTT TAA GCC-3′, and the reverse primer was 5′-dGGC TTA AAG GCC ATT GGT ACG TGA ATG ATG TAA AGA TCC-3′. The mutation was verified by dideoxysequencing. The mutant enzyme was overexpressed in *Escherichia coli* C41(DE3) cells in LB-Miller medium (BD Diagnostics) by the addition of isopropyl 1-thio-β-D-galactopyranoside (1 mM final concentration) at inoculation. The cells were grown for 20 h at 37 °C, harvested by centrifugation, and resuspended in buffer A (20 mM Tris (pH 8.6)) supplemented with 1 mg/ml lysozyme and 1 μg/ml DNase I (Roche Applied Science). The cells were lysed by sonication, and the protein in the soluble fraction was purified using a DEAE-Sepharose column with a linear salt gradient using buffer A and buffer B (20 mM Tris (pH 8.6), 250 mM NaCl). The mutant enzyme eluted at around 60 mM NaCl. Fractions containing the mutant were identified by SDS-PAGE analysis and pooled, and the final imidazole concentration was adjusted to 20 mM using buffer C (20 mM Tris (pH 7.9), 400 mM imidazole, 500 mM NaCl). The pooled fractions were then applied to a HisTrap FF column (5 ml), and the enzyme was purified by stepwise elution using 50% buffer C and 50% buffer D (20 mM Tris (pH 7.9), 20 mM imidazole, 500 mM NaCl). The purity of the protein was assessed by SDS-PAGE, and the protein concentration was determined by a Bradford protein assay using bovine serum albumin as a standard. The reductase activity of the pooled fractions after each chromatographic step was measured by the fluorimetric assay described under "Kinetic Analysis" using 1 μM 5α-DHT and 7.5 μM NADPH as substrates. The mutant was obtained in a 65% yield.

Enzymatic Synthesis of Radiolabeled Steroids—[^{14}C]5β-DHT was enzymatically synthesized from [^{14}C]testosterone by wild type (WT) AKR1D1. The reaction contained 100 mM potassium phosphate buffer (pH 6.0), 5% acetonitrile, 5% ethanol, 400 μM NADPH, 40 μM [^{14}C]testosterone (50 mCi/mmol), and 57.6 μg AKR1D1 in a final volume of 1 ml. The reaction was incubated at 37 °C for 1 h to achieve complete consumption of testosterone. [^{3}H]5α-Androstane-3,17-dione was enzymatically synthesized from [^{3}H]androsterone by AKR1C9. The reaction contained 100 mM K_2HPO_4, 5% ethanol, 2.2 mM NAD^+, 0.9 μM [^{3}H]androsterone (54 Ci/mmol), and 15 μg of AKR1C9 in a final volume of 1 ml. The reaction was incubated at 37 °C for 1 h to achieve complete consumption of androsterone. [^{14}C]20α-Hydroxyprogesterone (20α-OHP) was synthesized from [^{14}C]progesterone by AKR1C1. The reaction contained 100 mM potassium phosphate buffer (pH 6.0), 4% ethanol, 950 μM NADPH, 76 μM [^{14}C]progesterone (55 mCi/mmol), and 180 μg of AKR1C1 in a final volume of 0.5 ml. The reaction was incubated at 37 °C for 2 h with ~75% conversion of progesterone. [^{14}C]20α-OHP required further purification from the unreacted progesterone by chromatography (silica 60, CH_2Cl_2/ether, 60:5 (v/v)). After incubation, all reactions were quenched and extracted with ethyl acetate. The purity of the synthesized steroids was assessed by TLC as described below. The specific radioactivity of the synthesized substrates was based on the value for the starting material.

Product Identification by TLC—The 5β-reductase activity of the AKR1D1 E120H mutant was examined using testosterone, progesterone, and Δ^4-Adione as substrates with NADPH as cofactor. The ketosteroid reductase activity of the E120H mutant was examined using 5α-DHT, 5β-DHT, androsterone, Δ^4-Adione, and progesterone as substrates and NADPH as cofactor. The reactions were performed in 200-μl systems containing 100 mM potassium phosphate buffer (pH 6.0), 4% acetonitrile, 200 μM NADPH, 2.8 μg of AKR1D1 E120H, and one of the following substrates: 5 μM [^{14}C]testosterone (20 mCi/mmol), 5 μM [^{14}C]progesterone (5 mCi/mmol), 2 μM [^{14}C]Δ^4-Adione (48 mCi/mmol), 1 μM [^{3}H]5α-DHT (495 mCi/mmol), 1.9 μM [^{14}C]5β-DHT (50 mCi/mmol), or 5 μM [^{3}H]androsterone (530 mCi/mmol).

The hydroxysteroid oxidase activity of the E120H mutant was evaluated using androsterone, testosterone, 5α-DHT, 5β-DHT, 17β-estradiol, and 20α-OHP as substrates, using $NAD(P)^+$ as cofactor. The reactions were performed in 200-μl systems containing 100 mM potassium phosphate buffer (pH 7.0), 4% acetonitrile, 2.2 mM NAD^+ (200 μM $NADP^+$ for 5α-DHT and androsterone oxidation), 2.8 μg of AKR1D1 E120H, and one of the following substrates: 5 μM [^{3}H]androsterone (530 mCi/mmol), 5 μM [^{14}C]testosterone (20 mCi/mmol), 5 μM [^{3}H]5α-DHT (580 mCi/mmol), 5 μM [^{14}C]5β-DHT (13 mCi/mmol), 2 μM [^{14}C]17β-estradiol (53 mCi/mmol), or 5 μM [^{14}C]20α-OHP (7.4 mCi/mmol).

All reactions were incubated at 37 °C and quenched by 1 ml of ethyl acetate at different time intervals. Control reactions that contained the same components as the reaction mixture less enzyme were performed for each substrate using a 60-min incubation. The aqueous phase was extracted with ethyl acetate, and the extracts were applied to an LK6D Silica 60 TLC plate (Whatman), and the radioactive peaks were detected by a TLC-linear analyzer (Bioscan Imaging Scanner system 200-IBM with AutoChanger 3000; Bioscan). Products of the reactions were identified by co-chromatography with authentic synthetic standards. The chromatograms for reactions containing 5α-DHT, Δ^4-androstene-3,17-dione, androsterone, or 17β-estradiol were developed three times in CH_2Cl_2/ether (110:10, v/v). The chromatograms for reactions containing testosterone or 5β-DHT were developed twice in toluene/acetone (80:20, v/v). The chromatograms for reactions containing progesterone or 20α-OHP were developed once in CH_2Cl_2/ethyl acetate (80:20, v/v).

Kinetic Analysis—Reductase activity was monitored fluorimetrically by measuring the disappearance of the NADPH signal (λ_{ex} = 340 nm, λ_{em} = 460 nm) in 1-ml systems containing 100 mM potassium phosphate buffer (pH 6.0), 4% acetonitrile, 7.2 μM NADPH, and varied concentrations of steroid (0.2–60 μM) at 37 °C. The oxidase activity was monitored fluorimetrically by measuring the appearance of NADH signal (λ_{ex} = 340 nm, λ_{em} = 460 nm) in 1-ml systems containing 100 mM potassium phosphate buffer (pH 7.0), 4% acetonitrile, 2.3 mM NAD^+, and varied concentrations of steroid (0.2–60 μM) at 37 °C. Reactions were initiated by the addition of enzyme and were

corrected for the non-enzymatic rate. Kinetic constants were calculated by fitting the initial velocity data to either the Michaelis-Menten equation or the modified Michaelis-Menten equation with a term for substrate inhibition (Equation 1) using GraFit (Erithacus Software Ltd.). The iterative fits gave estimates of the steady-state kinetic parameters, mean ± S.E.

$$v = \frac{V_{max}[S]}{K_m + [S] + [S]^2/K_i} \quad \text{(Eq. 1)}$$

Crystallography—Four different complexes were obtained for the E120H mutant (E120H·$NADP^+$, E120H·$NADP^+$·epiA, E120H·$NADP^+$·Δ^4-Adione, and E120H·$NADP^+$·5β-DHT) using the hanging drop vapor diffusion method at 4 °C. Besides the steroid, drops typically contained 3.0 μl of protein solution (10 mg/ml AKR1D1 E120H mutant, 2.0 mM $NADP^+$, and 10 mM Tris-HCl (pH 7.4)) and 3.0 μl of well solution (0.1 M Tris-HCl (pH 7.0–7.7), 14–20% (w/v) polyethylene glycol 4000, and 10% isopropyl alcohol). Steroid solutions of 100 mM were prepared in isopropyl alcohol and added to the protein solution in co-crystallization trials or to the soaking solution to obtain the desired steroid concentration without adjustment of the final isopropyl alcohol concentration to a constant value. Crystals appeared and grew to a suitable size for diffraction in approximately a week. The ternary complex of E120H·$NADP^+$·epiA was obtained by co-crystallization in the presence of 2 mM 5α-DHT, and the E120H·$NADP^+$·Δ^4-Adione complex was obtained in the presence of 2 mM testosterone. The steroids in the structures were different from those used in co-crystallization due to substrate turnover (see "Results"). The E120H·$NADP^+$·5β-DHT complex was obtained by soaking the binary complex E120H·$NADP^+$ in the mother liquor augmented with 5 mM $NADP^+$ and 5 mM 5β-DHT for 6 h. Prior to flash-cooling, crystals were soaked for 5 min in a 16% (w/v) Jeffamine ED-2001 cryoprotective solution containing 2 mM $NADP^+$ and 2 mM steroid to maintain full occupancy of the steroid ligand. Diffraction data of the E120H·$NADP^+$, E120H·$NADP^+$·Δ^4-Adione, and the E120H·$NADP^+$·5β-DHT complexes were collected at beamline 24-ID-C (λ = 0.979 Å) of the Advanced Photon Source at Argonne National Laboratory (Argonne, IL). The data of the E120H·$NADP^+$·epiA complex were collected at beamline X29 (λ = 1.075 Å) of the National Synchrotron Light Source at Brookhaven National Laboratory (Upton, NY). All crystals are of the $P2_12_12_1$ space group with unit cell parameters $a = 50.03$, $b = 109.71$, and $c = 129.34$ Å, similar to those of the WT AKR1D1 (10). The asymmetric unit of the unit cell contains two monomers of the E120H mutant. Data were integrated and scaled with HKL2000 and Scalepack (18). Data collection and reduction statistics are reported in Table 1 for all complexes.

The structure of the E120H·$NADP^+$ complex was solved by molecular replacement performed with PHASER (19) from the CCP4 suite using the coordinates of the WT AKR1D1·$NADP^+$ binary complex (PDB code 3BV7) (10) less ligand and solvent molecules as a search model. The structures of ternary complexes E120H·$NADP^+$·epiA, E120H·$NADP^+$·Δ^4-Adione, and E120H·$NADP^+$·5β-DHT were solved by the difference Fourier method using the E120H·$NADP^+$ complex as a starting model. The programs CNS (20), PHENIX (21), and COOT (22) were used for refinement and model fitting. $NADP^+$ and steroids were built into the electron density map at the final stage of refinement. The quality of the models was verified with Molprobity and PROCHECK. PROCHECK identified residue Thr^{224} in both monomers in all of the AKR1D1 E120H complexes in the disallowed region. The refinement statistics are reported in Table 1.

RESULTS

Loss of 5β-Reductase Activity—The E120H mutation effectively abolished the 5β-reductase activity found in WT AKR1D1. No 5β-reduced product was observed with the AKR1D1 E120H mutant when [^{14}C]testosterone, [^{14}C]progesterone, or [^{14}C]Δ^4-Adione was employed as the substrate in the presence of NADPH after a 1-h-long incubation at 37 °C. The limit of detection of the assay was 0.2 pmol/min, and we estimated that if any residual activity remained, it was less than 0.8% of wild-type enzyme.

3β-Hydroxysteroid Dehydrogenase Activity of AKR1D1 E120H Mutant—The ability of the E120H mutant to act as an HSD was examined for the reduction of 3-, 17-, and 20-ketosteroids and the oxidation of the corresponding hydroxysteroids (Scheme 3). Enzyme activity was monitored by measuring the change of fluorescence emission of the cofactor to generate steady-state kinetic parameters. Concurrently, reactions were performed with radiolabeled steroid substrates so that product profiles of the reactions could be ascertained. Product identity was achieved by TLC by measuring co-migration of the radiolabeled peaks with authentic synthetic standards.

The E120H mutant was expected to function as a 3α-HSD like the AKR1C enzymes but to maintain a preference for 3-ketosteroids with a 5β-configuration because these are produced by WT AKR1D1. To our surprise, the E120H mutant acted predominantly as a 3β-HSD that preferred steroids with a 5α-configuration over those with a 5β-configuration. In ketosteroid reduction, the mutant stereospecifically reduced 5α-DHT to 5α-androstane-3β,17β-diol (Fig. 1) with a catalytic efficiency of 2.1×10^5 M^{-1} s^{-1}, which was 10-fold higher than that for the reduction of 5β-DHT, which has the opposite configuration (Table 2). For hydroxysteroid oxidation, the mutant oxidized the 3β-hydroxysteroid, epiA, to 5α-androstane-3,17-dione with a catalytic efficiency of 1.3×10^5 M^{-1} s^{-1}, which was at least 15-fold higher than the catalytic efficiency of the other tested hydroxysteroids regardless of the configuration of the steroid A/B ring junction and the position of catalysis (3-, 17-, or 20-position) (Table 3).

Comparison of AKR1D1 E120H Mutant with AKR1C Enzymes—AKR1C enzymes perform ketosteroid reduction and exhibit similar catalytic efficiencies for the reduction of 5α- and 5β-DHT and preferably form the 3α-hydroxysteroid over the 3β-hydroxysteroid (23, 24). The exception is AKR1C1, which reduces 5α-DHT to a mixture of 3α- and 3β-isomers in a 1:3 ratio. The AKR1D1 E120H mutant exhibited superior specificity and efficiency for the reduction of 5α-DHT to yield 5α-androstane-3β,17β-diol than observed with AKR1C1 (Table 2). The E120H mutant produced only the 3β-isomer and had a

TABLE 1
Data collection and refinement statistics

Structure	E120H·NADP$^+$	E120H·NADP$^+$·epiA	E120H·NADP$^+$·Δ^4-Adione	E120H·NADP$^+$·5β-DHT
Data collection				
Resolution range (Å)	50.0–1.89	50.0–1.64	50.0–1.82	50.0–1.83
Total reflections	286,303 (25,145)[a]	342,248 (32,768)[a]	282,951 (30,478)[a]	295,651 (28,129)[a]
Unique reflections measured	57,071 (5350)[a]	86,051 (8402)[a]	58,850 (6220)[a]	58,578 (5985)[a]
R_{merge}[b]	0.099 (0.43)[a]	0.055 (0.23)[a]	0.069 (0.46)[a]	0.087 (0.405)[a]
$I/\sigma(I)$	13.5 (3.0)[a]	23.0 (5.5)[a]	20.7 (3.2)[a]	15.5 (3.8)[a]
Completeness (%)	98.9 (94.3)[a]	97.4 (96.4)[a]	90.7 (96.9)[a]	92.0 (95.7)[a]
Refinement statistics				
Reflections used in refinement/test set	54,659/2754	84,885/4299	56,182/2845	56,863/2892
R/R_{free}[c]	0.168/0.211	0.184/0.219	0.191/0.246	0.173/0.218
Protein atoms[d]	5256	5256	5256	5256
Water molecules[d]	622	596	504	550
NADP$^+$ molecules[d]	2	2	2	2
Chloride ion[d]	3	4	1	2
Steroid molecules[d]		2	2	2
Root mean square deviations				
Bond lengths (Å)	0.006	0.004	0.006	0.007
Bond angles (degrees)	1.0	1.0	1.1	1.1
Overall *B*-factor (Å^2)	21	21	22	21
Cofactor *B*-factor (Å^2)	12	13	14	13
Steroid *B*-factor (Å^2)		28	41	43
Ramachandran statistics[e]				
Allowed (%)	90.4	90.0	89.0	90.2
Additionally allowed (%)	9.3	9.6	10.7	9.4
Generously allowed (%)	0.0	0.0	0.0	0.2
Disallowed (%)	0.3	0.3	0.3	0.2

[a] The number in parentheses refers to the outer 0.1-Å shell of data.
[b] $R_{merge} = \Sigma|I - \langle I\rangle|/\Sigma I$, where I is the observed intensity and $\langle I\rangle$ is the average intensity calculated for replicate data.
[c] Crystallographic *R*-factor, $R = \Sigma(|F_o| - |F_c|)/\Sigma|F_o|$ for reflections contained in the working set. Free *R*-factor, $R_{free} = \Sigma(|F_o| - |F_c|)/\Sigma|F_o|$ for reflections contained in the test set excluded from refinement. $|F_o|$ and $|F_c|$ are the observed and calculated structure factor amplitudes, respectively.
[d] Per asymmetric unit.
[e] Ramachandran statistics were calculated with PROCHECK (42). Thr^{224} in both monomers of all the AKR1D1 E120H complexes was found in the disallowed region.

catalytic efficiency for 5α-DHT that was 400-fold greater than that observed for the same reduction reaction catalyzed by AKR1C1. In addition, the k_{cat}/K_m value for the reduction of 5α-DHT catalyzed by the E120H mutant was about 15-fold greater than that observed for the reduction of this steroid to the opposite stereoisomer, 5α-androstane-3α,17β-diol, catalyzed by AKR1C2. The values obtained with the mutant were similar to that observed for the reduction of 5α-DHT to 5α-androstane-3α,17β-diol catalyzed by AKR1C4, the most efficient human AKR1C enzyme (23).

Functional Promiscuity of E120H Mutant as Hydroxysteroid Dehydrogenase—The E120H mutant also exhibited subsidiary functional promiscuity by catalyzing the reduction of select 3- and 17-ketosteroids and oxidation of 3α/β-, 17β-, and 20α-hydroxysteroids with different stereochemical outcomes.

In the reduction direction, the AKR1D1 E120H mutant nonstereospecifically reduced the 3-ketosteroid 5β-DHT to a mixture of 5β-androstane-3α,17β-diol and 5β-androstane-3β,17β-diol in a 4:1 ratio with a catalytic efficiency 10-fold lower than that observed with 5α-DHT (supplemental Fig. S1 and Table 2). Interestingly, the stereopreference for the 5β-DHT reduction catalyzed by the E120H mutant is now consistent with the stereopreference of the AKR1C enzymes, which greatly favors the production of the 3α-isomer when the substrate has the 5β-configuration (24). The E120H mutant also reduced 17-ketosteroids and converted androsterone to 5α-androstane-3α,17β-diol and Δ^4-Adione to testosterone, but the reaction rates were too slow to be captured by the fluorimetric assay (supplemental Fig. S2).

In the oxidation direction, the E120H mutant slowly converted 3-hydroxysteroids with a 3α,5α-configuration (supplemental Fig. S3) or a 3α,5β- or 3β,5β-configuration to the corresponding 3-ketosteroids with similar catalytic efficiencies. Their catalytic efficiencies were much lower than that of the oxidation of epiA, which contains the preferred 3β,5α-configuration (Table 3). The E120H mutant also oxidized 17β-hydroxysteroids and converted 5α-DHT to 5α-androstane-3,17-dione, 17β-estradiol to estrone, testosterone to Δ^4-Adione, and 5β-DHT to 5β-androstane-3,17-dione (supplemental Fig. S4 and Table 3). Oxidation of 5α-DHT at the 17β-position exhibited slightly higher catalytic efficiency than that observed for the oxidation of the 3-hydroxysteroids except for epiA. The oxidation of the 17β-position of 5α-DHT was also preferred over the oxidation of the 17β-position of 5β-DHT and gave a catalytic efficiency that was 50-fold higher. The E120H mutant also catalyzed a very slow oxidation of 20α-hydroxyprogesterone to progesterone, but accurate kinetic parameters were not obtained due to the slow reaction rate and substrate inhibition (supplemental Fig. S5 and Table 3). The catalytic efficiencies of these minor oxidative activities on the 3α/β-, 17β-, and 20α-hydroxysteroids were 20 – 800-fold lower than that obtained for the oxidation of epiA catalyzed by the 3β-HSD activity of the E120H mutant.

Overview of Structure of E120H Mutant—We determined the crystal structures of the E120H mutant in complex with NADP$^+$, NADP$^+$ and epiA, NADP$^+$ and Δ^4-Adione, and NADP$^+$ and 5β-DHT to develop a structural explanation for the observed change of function. Each complex contained two monomers of the E120H mutant in the asymmetric unit. Monomer B typically exhibited lower thermal *B*-factors compared with monomer A, especially in the loop regions (Loop A, Ile^{119}–Leu^{147}; Loop B, Tyr^{219}–Leu^{238}; Loop C,

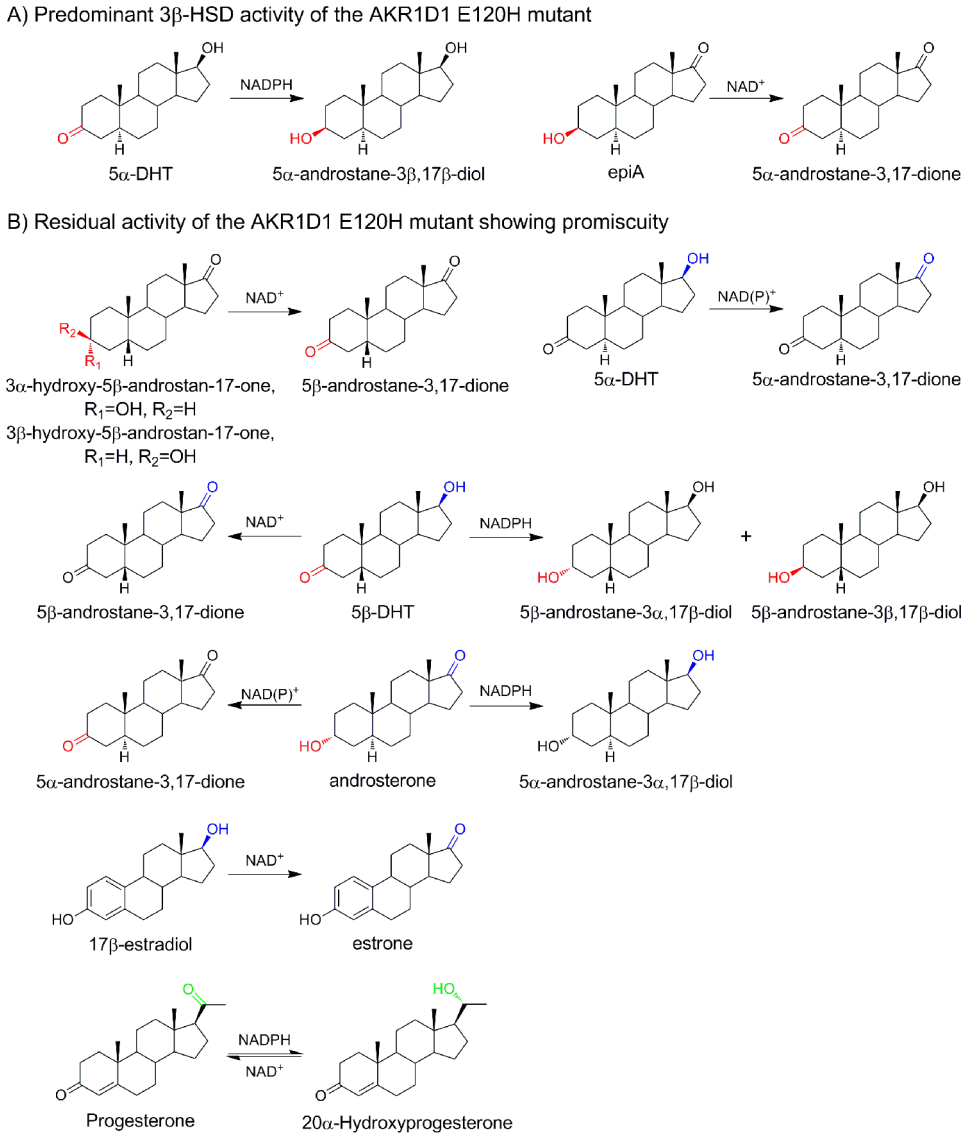

SCHEME 3. **Representative reactions monitored to determine substrate specificity of the AKR1D1 E120H mutant.** The reactive centers in the steroid are shown in *red* (3-position), *blue* (17-position), and *green* (20-position).

Leu^{302}–Tyr^{326}), although no significant conformational differences were evident between the two monomers. This finding is consistent with the reported structure of WT AKR1D1 (10). The E120H mutation did not perturb the overall structure of the protein. The root mean square deviations between the AKR1D1·NADP$^+$·cortisone structure (PDB code 3CMF) and the structures of the four complexes of the E120H mutant were within 0.18 Å for the 325 residues in monomer B and were similar to the root mean square deviations when the individual mutant complexes were compared (0.09–0.12 Å). When the AKR1D1·NADP$^+$·HEPES complex structure is compared with the AKR1D1 E120H·NADP$^+$ complex structure, the similarity in the structures is apparent (Fig. 2*A*). The His^{120} residue in the E120H mutant adopts the same conformation as the Glu^{120} residue in WT AKR1D1. The two residues were essentially superimposed with each other at their backbones and side chains up to the C-γ atom (Fig. 2*B*). Cofactor binding was undisturbed by the mutation, as expected, due to the lack of direct interaction between the cofactor and Glu^{120}. NADP$^+$ maintained the same hydrogen bond network as well as the salt link between Arg^{279} and the 2′-phosphate of AMP moiety that is responsible for the tight binding of NADPH (10, 25). The positioning of the nicotinamide ring of the cofactor in the central active site cavity retained the same location as found in WT AKR1D1.

E120H·NADP$^+$ Complex—The E120H·NADP$^+$ complex was obtained by co-crystallization with NADP$^+$. In the binary complex, a water molecule occupied the oxyanion site through hydrogen-bonding to Tyr^{58} and His^{120} (Fig. 2*B*). In the absence of a steroid ligand, Trp^{230} swung into the steroid binding channel, triggering a slight movement of Loop B.

E120H·NADP$^+$·epiA Complex—The E120H·NADP$^+$·epiA complex was obtained by co-crystallization with 5α-DHT. Simulated annealing omit maps indicated that two androgens distinct from 5α-DHT were bound in the two monomers of the complex. EpiA agreed well with the electron density map in monomer B with lower average *B*-factors (Fig. 3*A*), whereas 5α-androstane-3β,17β-diol best depicted the map in monomer

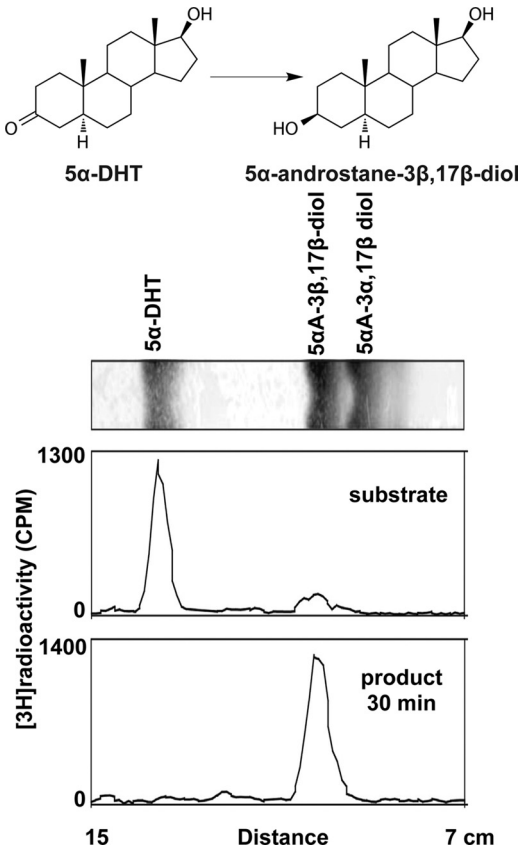

FIGURE 1. **Identification of the products obtained by the E120H mutant catalyzed reduction of 5α-DHT.** The mutant stereospecifically reduced 5α-DHT to 5α-androstane-3β,17β-diol. *5αA-3α,17β-diol*, 5α-androstane-3α,17β-diol; *5αA-3β,17β-diol*, 5α-androstane-3β,17β-diol. *Distance*, plate length. The bottom of the plate is marked as zero.

A (supplemental Fig. S6). An assay mimicking the crystallization condition was performed and showed that 5α-DHT oxidoreduction occurred during the crystallization process and produced a mixture of products that included epiA, 5α-androstane-3β,17β-diol, and 5α-androstane-3,17-dione (supplemental Fig. S4). The electron density map of the ligand identified the steroid that occupied the active site most frequently. Despite the difference in functional groups at the C17-position, the two 3β,5α-tetrahydrosteroids occupied identical positions in the steroid binding channel. The structure of monomer B with epiA was selected to represent the complex. EpiA was oriented with the A-ring toward the active site center, placing the 3β-hydroxy group in the oxyanion site through interactions with Tyr^{58} and His^{120}. Trp^{230} receded from the steroid channel, packing against the α-face of the steroid. The distance of 3.2 Å between the C3-position of the steroid and the C4 atom on the nicotinamide ring was within a suitable distance for hydride transfer. The steroid α-face was directed toward the *re*-face of the cofactor, which allowed oxidoreduction of the 3β,5α-reduced hydroxysteroid, consistent with the observed stereopreference of the E120H mutant. Compared with WT AKR1D1, the E120H mutant bound steroids with an opposite facial orientation, and the oxyanion site in the mutant was shifted "upward" by 1.5 Å (Fig. 3*B*). This movement placed the C3-position of the steroid in the E120H mutant at a position that could be superimposed on the oxyanion site in the AKR1C enzymes, illustrated by the position of the 3-ketone group in testosterone in the AKR1C9·$NADP^+$·testosterone complex (PDB code 1ASF) (Fig. 3*C*).

E120H·$NADP^+$·Δ^4-Adione Complex—The E120H·$NADP^+$·Δ^4-Adione was obtained by co-crystallization with testosterone. Akin to the phenomenon observed with the E120H·$NADP^+$·epiA complex, oxidation of the 17β-hydroxy group of testosterone was observed. Δ^4-Adione was found in monomer B of the complex with lower average *B*-factors (Fig. 4*A*), whereas testosterone was found in monomer A (supplemental Fig. S7). Both Δ^4-3-ketosteroids occupied identical positions in the steroid binding channel. Δ^4-Adione bound to the steroid binding channel with its A-ring, rather than the D-ring, pointing toward the active site, placing the 3-ketone group at the oxyanion site in a nonproductive orientation. Despite the structural resemblance between Δ^4-Adione and epiA, the binding orientation of Δ^4-Adione resembles 5β-DHT by orientating its β-face toward the cofactor (*i.e.* the steroid face has been flipped). In the WT AKR1D1·$NADP^+$·testosterone structure, testosterone was bound perpendicular to the steroid binding channel in an alternative binding pocket, which is responsible for the reported substrate inhibition of WT AKR1D1 (Fig. 4*B*) (26). In the E120H mutant structure, testosterone was bound in the steroid binding channel, although the mutation did not disrupt the alternative binding pocket. Substrate inhibition observed for testosterone oxidation catalyzed by the mutant could be elicited either by steroid fitting into the alternative binding pocket as in the wild type AKR1D1 or binding nonproductively in the steroid channel so that its A-ring is in proximity with the cofactor.

E120H·$NADP^+$·5β-DHT Complex—The E120H·$NADP^+$·5β-DHT complex was obtained by soaking 5β-DHT into the E120H·$NADP^+$ complex. Although 5β-DHT is a substrate for the E120H mutant, no turnover was observed due to its low catalytic efficiency and relatively short incubation time with the enzyme. The steroid nucleus of 5β-DHT occupied a similar position in the steroid binding channel as epiA with the A-ring approaching the cofactor (Fig. 5*A*). However, 5β-DHT bound distally from the catalytic site and instead a water molecule was anchored to the oxyanion site. This represents a non-productive binding mode witnessed in monomer A of the AKR1D1·$NADP^+$·5β-DHP complex (PDB code 3CAV) (25), which resembles a conformation that precedes steroid product release from the WT enzyme. The β-face of 5β-DHT was directed toward the cofactor, retaining the same orientation utilized for steroid 5β-reduction and coincides with the stereopreference of the mutant to produce the 3α,5β-reduced steroid product from 5β-DHT. Slight movements of Trp^{230} and Tyr^{132} were observed to accommodate the flip of the C18 and C19 angular methyl groups. In the WT AKR1D1·$NADP^+$·5β-DHT structure (PDB code 3DOP) (27), the steroid was also bound through a water molecule; however, the 17β-hydroxy group of the steroid was directed toward the oxyanion site instead of the 3-ketone group (Fig. 5*B*).

DISCUSSION

Glutamate-Histidine Substitution Controls 5β-Reductase and HSD Activity—Engineered enzymes usually exhibit crippled catalytic efficiency and partially retain their original activ-

TABLE 2
Kinetic constants for 3-ketosteroid reduction catalyzed by the E120H mutant and AKR1C2

Substrate	Product specificity	k_{cat}	K_m	K_i	k_{cat}/K_m
		$\times 10^{-3}\ s^{-1}$	μM	μM	$\times 10^{2}\ M^{-1}\ s^{-1}$
E120H					
5α-DHT	3β	33.8 ± 0.8	0.16 ± 0.02	3.9 ± 0.2	2100
5β-DHT	3α (80%), 3β (20%)	26.8 ± 0.7	1.5 ± 0.1	47.1 ± 3.6	180
AKR1C1					
5α-DHT[a]	3α (25%), 3β (75%)[b]	NA[c]	NA		4.8
AKR1C2					
5α-DHT	3α (95%), 3β (5%)[b]	123 ± 3	8.2 ± 0.8		150
5β-DHT	3α (88%), 3β (11%)[d]	21.7 ± 0.3	2.0 ± 0.2		110

[a] AKR1C1 failed to display saturation kinetics due to the limit of substrate solubility. The k_{cat}/K_m values were thus estimated from the slope of the initial velocity-substrate concentration curve.
[b] Data from Refs. 23 and 28. The ratio was determined at pH 7.0 using radiometric assays.
[c] NA, not available.
[d] Data from Ref. 24. The ratio was determined at pH 7.0 by LC-MS.

TABLE 3
Kinetic constants for hydroxysteroid oxidation catalyzed by the E120H mutant and AKR1C2

Substrate	Substrate stereospecificity	k_{cat}	K_m	K_i	k_{cat}/K_m
		$\times 10^{-3}\ s^{-1}$	μM	μM	$\times 10^{2}\ M^{-1}\ s^{-1}$
E120H					
Androsterone	3α, 5α	47 ± 2	27.5 ± 3.1		17
epiA	3β, 5α	253 ± 8	1.9 ± 0.3		1300
3α-Hydroxy-5β-androstan-17-one	3α, 5β	125 ± 3	36.4 ± 2.3		34
3β-Hydroxy-5β-androstan-17-one	3β, 5β	43 ± 2	15.3 ± 2.2		28
5α-DHT	17β	5.8 ± 0.3	0.8 ± 0.1	36.7 ± 7.2	73
17β-Estradiol	17β	5.87 ± 0.07	2.8 ± 0.1		21
Testosterone	17β	0.77 ± 0.05	1.8 ± 0.3	40.4 ± 7.9	4.2
5β-DHT	17β	0.85 ± 0.05	5.7 ± 1.2		1.5
20α-Hydroxyprogesterone[a]	20α	>0.3	<0.52	Yes	NA[b]
AKR1C2					
Androsterone	3α, 5α	21.7 ± 0.8	9.3 ± 0.9		23
epiA[a]	3β, 5α	~0.07	<5.86		NA
3α-Hydroxy-5β-androstan-17-one	3α, 5β	14 ± 1	29.0 ± 4.2		4.9
3β-Hydroxy-5β-androstan-17-one	3β, 5β	0.183 ± 0.008	9.4 ± 1.2		0.2
5α-DHT	17β	0.28 ± 0.02	15.3 ± 3.3		0.19
17β-Estradiol	17β	1.6 ± 0.1	6.2 ± 1.2		2.6
Testosterone	17β	0.348 ± 0.008	17.3 ± 1.1		0.2
5β-DHT[a]	17β	0.112 ± 0.005	<1.89		NA
20α-Hydroxyprogesterone	20α	2.12 ± 0.05	6.0 ± 0.5		3.5

[a] Kinetic constants were not determined due to slow reaction rate.
[b] NA, not available.

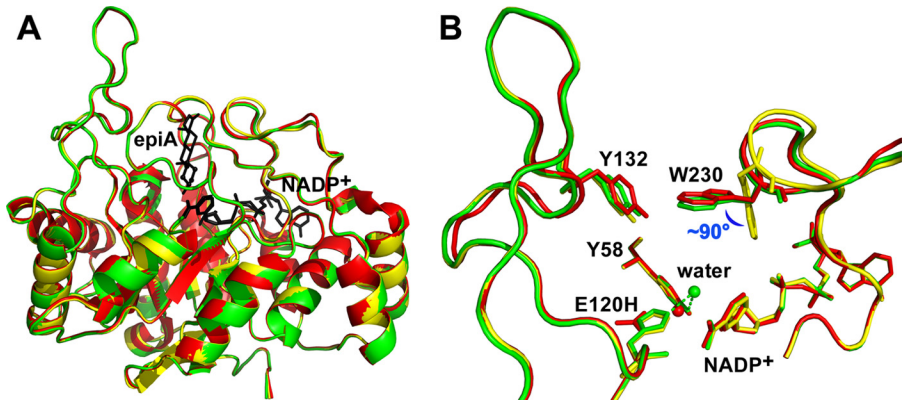

FIGURE 2. **Structure of the AKR1D1 E120H·NADP$^+$ binary complex.** Superposition of the overall structure (*A*) and active site (*B*) of the AKR1D1 E120H·NADP$^+$ (*green*), AKR1D1 E120H·NADP$^+$·epiA (*yellow*), and WT AKR1D1·NADP$^+$·HEPES complexes (*red*; PDB code 3BUV), showing that no significant conformational change was induced by the E120H mutation. NADP$^+$ and epiA molecules in *A* are *colored* in *black*. The steroid A-ring is shown in a *ball-and-stick representation*. In the binary complexes, a water molecule resides in the oxyanion site, and Trp^{230} swings 90° into the steroid binding channel. The *green dashed lines* indicate hydrogen bond interaction in the AKR1D1 E120H·NADP$^+$ complex with the water molecule. epiA was omitted from *B* for clarity. All structural figures were generated with PyMOL (Version 1.2r1 Schrödinger, LLC).

ity. Here we demonstrate that a single glutamate-to-histidine mutation in AKR1D1 eliminates its 5β-reductase activity and converts the enzyme into a proficient 3β-HSD. The stereopreference of the E120H mutant is different from most of the AKR1C enzymes except AKR1C1 (23, 28). The introduced 3β-HSD activity is much higher than observed with AKR1C1 and is comparable with and in some cases even higher than native 3β-HSDs in the short-chain dehydrogenase/reductase family (29). We have previously engineered 5β-reductase activity into rat 3α-HSD AKR1C9 by introducing the corresponding

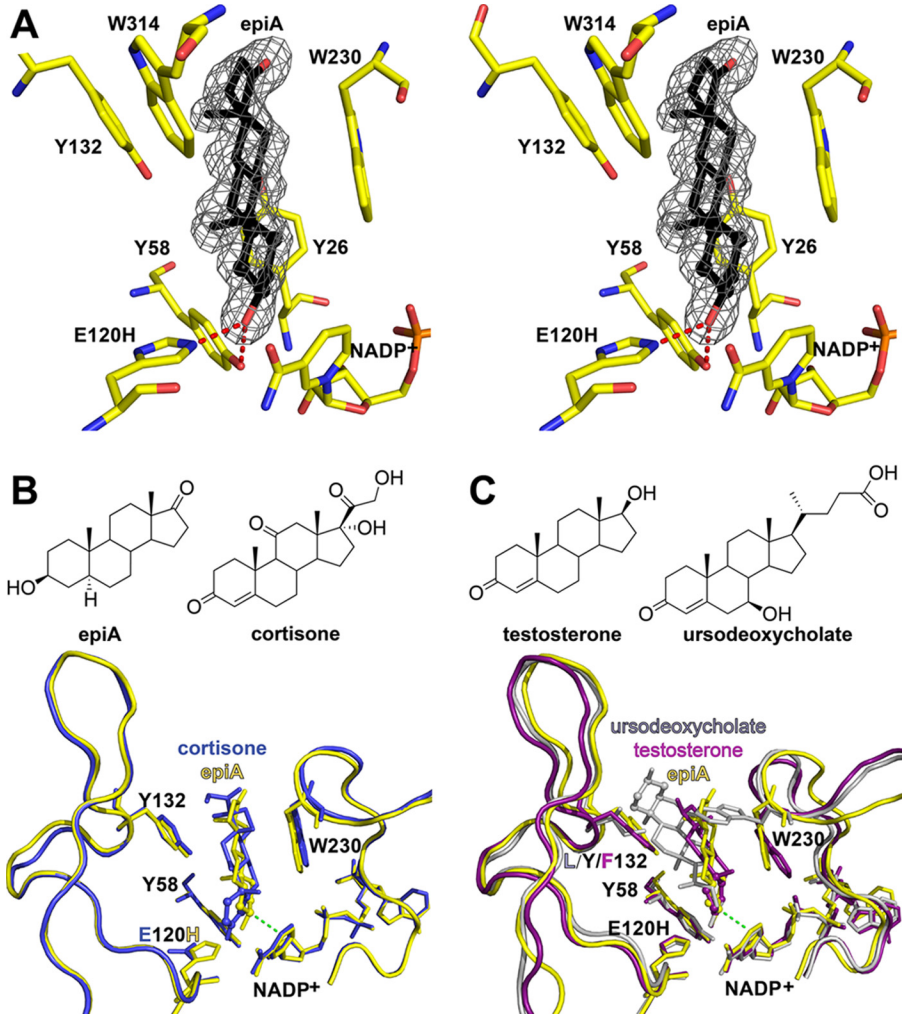

FIGURE 3. **Structure of the AKR1D1 E120H·NADP$^+$·epiA complex.** *A*, stereoviews of the simulated annealing omit map ($F_o - F_c$) of epiA contoured at 2.8 σ. Atoms are *colored-coded* as follows. *Yellow*, protein carbon; *black*, steroid carbon; *blue*, nitrogen; *red*, oxygen; *orange*, phosphorus. Hydrogen bonds are indicated by *red dashed lines*. The steroid A-rings are shown in *ball-and-stick representations*. *B*, superposition of AKR1D1 E120H·NADP$^+$·epiA (*yellow*) and WT AKR1D1·NADP$^+$·cortisone complex (PDB code 3CMF; *blue*). The AKR1D1 E120H mutation allows the C3 carbonyl to reside ~1 Å closer to the 4-pro-(*R*)-hydride on the nicotinamide ring. The trajectory of hydride transfer is indicated by a *green dashed line*. *C*, superposition of AKR1D1 E120H·NADP$^+$· (*yellow*), AKR1C2·NADP$^+$·ursodeoxycholate (PDB code 1IHI; *gray*), and AKR1C9·NADP$^+$·testosterone complex (PDB code 1ASF; *purple*). The testosterone 3-ketone group in AKR1C9 superimposed well with the 3-hydroxy group of epiA in the E120H mutant. Residues are *numbered* as in AKR1D1.

H120E mutation (numbering according to AKR1D1) (30). Characterization and kinetic analyses on the AKR1C9 H120E mutant showed that it exhibited moderate k_{cat} values ~0.005 s^{-1} and K_m values of ~20 μM toward four different Δ^4-3-ketosteroids, with catalytic efficiencies approximately one-thirtieth of the corresponding values of purified rat liver 5β-reductase AKR1D2 (31). The two studies complement each other and prove that the functional difference between AKR1D1 and AKR1C enzymes originates from a single glutamate-histidine substitution in the catalytic tetrad residue at position 120. Crystal structures of the AKR1D1 E120H mutant were determined to elucidate the structural basis for the change-of-function. Glu^{120} probably plays a dual role in determining the activity of AKR1D1 and the AKR1C enzymes; this residue controls the positional specificity of hydride transfer and facilitates double bond reduction.

Glu^{120} Controls Positional Specificity of Hydride Transfer—The E120H mutation does not disturb the overall structure of AKR1D1 or the position of the cofactor (Fig. 2). The histidine backbone in the E120H mutant is placed at essentially the same position as the glutamate residue in WT AKR1D1 (Fig. 3*B*). However, compared with the glutamate, which "swings" its side chain away from the steroid, the bulky imidazole ring of the histidine residue in the E120H mutant protrudes toward the catalytic center, adopting an orientation that closely resembles the conformation exhibited by His^{120} in the AKR1C enzymes (Fig. 3*C*). As a result, the steroid can no longer penetrate deep into the active site, and the oxyanion site in the mutant is shifted upward away from the cofactor to a location almost identical to the one it occupies in the AKR1C enzymes. This shift changes the recipient group for hydride transfer, from the C5-position to the C3-position of the steroid, and results in the loss of 5β-reductase activity and the gain of 3β-HSD activity. This phenomenon is reminiscent of what is seen in the short-chain dehydrogenase/reductase family, in which plant *Digitalis lanata* progester-

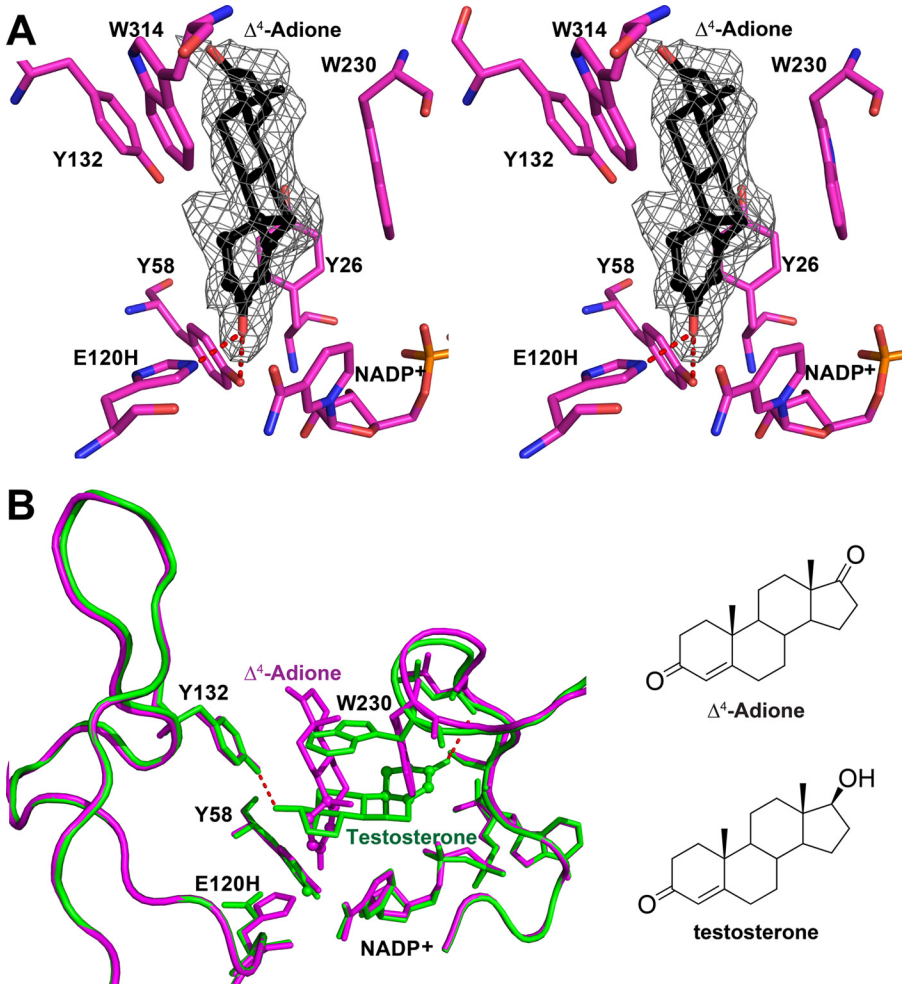

FIGURE 4. **Structure of the AKR1D1 E120H·NADP$^+$·Δ^4-Adione complex.** *A*, stereoviews of the simulated annealing omit map ($F_o - F_c$) of Δ^4-Adione contoured at 2.6 σ. Atoms are *color-coded* as described in the legend to Fig. 3, except the carbons of the AKR1D1 E120H mutant are *colored* in *magenta*. Hydrogen bonds are indicated by *red dashed lines*. The steroid A-rings are shown in *ball-and-stick representations*. *B*, superposition of AKR1D1 E120H·NADP$^+$·Δ^4-Adione (*magenta*) and WT AKR1D1·NADP$^+$·testosterone complex (PDB code 3BUR; *green*). The two steroid binding modes are perpendicular to each other, although the residues involved in hydrogen binding to testosterone in WT AKR1D1 do not move in the mutant.

one 5β-reductase corresponds to AKR1D1, and human 17β-HSD type I corresponds to the AKR1C enzymes. In these two short-chain dehydrogenase/reductases, the change from a 5β-reductase to a 17β-HSD is achieved by repositioning of a catalytic tyrosine. The shift of this tyrosine alters the depth of the steroid binding pocket so that either the steroid double bond or ketone group is positioned for reduction (32). However, in the short-chain dehydrogenase/reductase family, relocation of the catalytic tyrosine is accompanied by significant sequence and structural changes, whereas in the AKR family, a single glutamate-histidine substitution easily shifts the position of the steroid without rearrangement of the catalytic site.

Catalytic Role of Glu^{120}—The AKR1D1 E120A mutation allows steroid penetration in the active site but eradicates both 5β-reductase and HSD activity.[3] The H120A mutation in AKR1C9 also exhibits diminished 5β-reductase activity compared with the H120E mutant (30). These findings imply that the glutamate residue plays a role in the chemical mechanism of 5β-reduction. Studies on AKR1C9 H120E mutant show that the 5β-reductase activity is abolished by the Y58F/H120E double mutation but not by the H120A mutation, indicating that Glu^{120} greatly facilitates the reaction but is not obligatory for catalysis (30). The pH-rate dependence of these AKR1C9 mutants confirms that Tyr^{58} is the general acid for 5β-reduction and suggests that Glu^{120} lowers the pK_b of the general acid by hydrogen bonding to Tyr^{58}, resembling the role played by the histidine residue in AKR1C9 (Scheme 2, *left*) (30). However, the crystal structure of AKR1D1 disagrees with this mechanism. The distance between Glu^{120} and Tyr^{58} of 4.3 Å is too long for a hydrogen bond to exist between these two residues. Instead, the structure suggests that Glu^{120} donates a superacidic hydrogen bond to the steroid C3 carbonyl group, which activates the α,β-unsaturated steroid double bond by stabilizing the enolic intermediate during hydride transfer (Scheme 2, *right*) (10). The common feature of the two mechanisms is that Glu^{120} aids 5β-reduction by promoting an acidic environment. Currently, there are no kinetic data to support either mechanism directly. Characterization of the other Glu^{120}

[3] J. E. Drury and T. M. Penning, unpublished data.

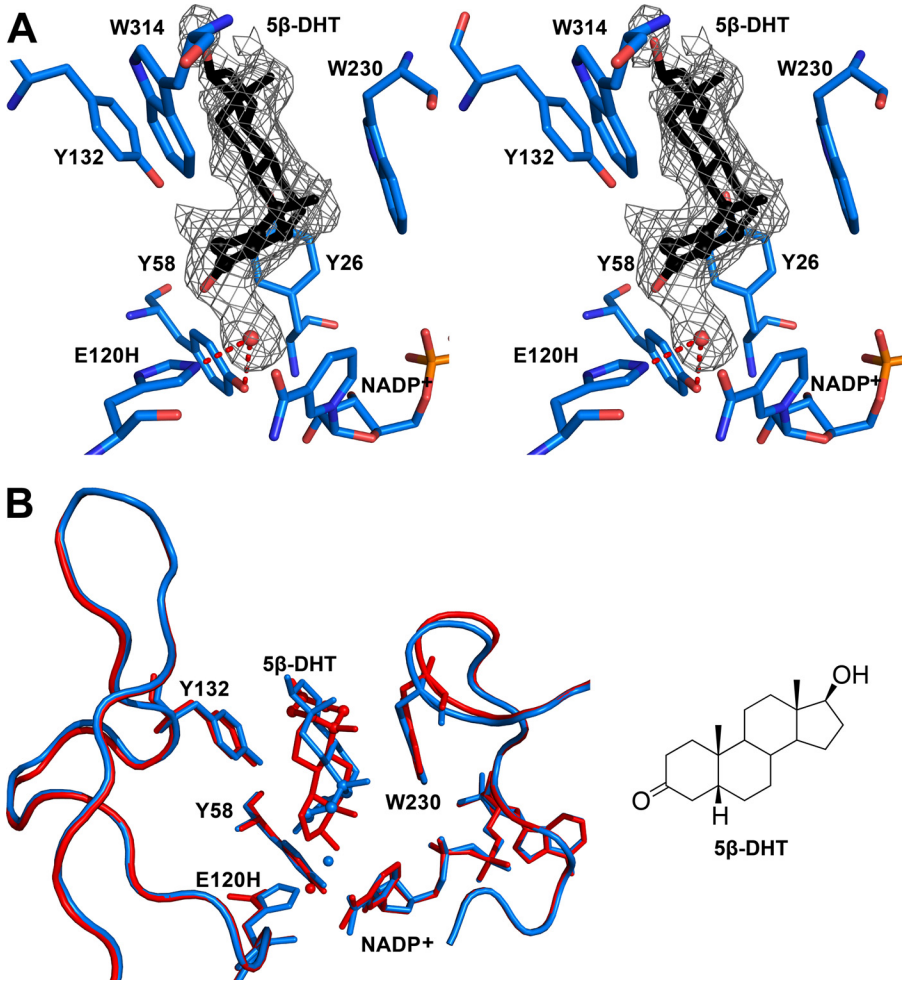

FIGURE 5. **Structure of the AKR1D1 E120H·NADP$^+$·5β-DHT complex.** *A*, stereoviews of the simulated annealing omit map ($F_o - F_o$) contoured at 2.5 σ. 5β-DHT adopts a non-productive binding mode in the active site, allowing a water molecule to occupy the oxyanion site. Atoms are *color-coded* as described in the legend to Fig. 3, except the carbons of the AKR1D1 E120H mutant are *colored* in *blue*. Hydrogen bonds are indicated by *red dashed lines*. The steroid A-rings are shown in *ball-and-stick* representations. *B*, superposition of E120H·NADP$^+$·5β-DHT (*blue*) and WT AKR1D1·NADP$^+$·5β-DHT complex (PDB code 3DOP; *red*). 5β-DHT binds with its A-ring approaching the oxyanion site in the AKR1D1 E120H mutant and with its D-ring approaching the oxyanion site in the WT AKR1D1. Water molecules are shown as *spheres*. Only monomer B is shown.

mutations, including E120D, E120Q, and E120N, will probably unveil the catalytic property of this residue. A similar mechanistic problem existed for *Pseudomonas* Δ^5-3-ketosteroid isomerase, in which Tyr^{14} functions as the general acid and Asp^{38} acts as the general base, but the role of a neighboring Asp^{99} was uncertain. This residue could be either hydrogen-bonded directly to the steroid substrate (33, 34) or to Tyr^{14} to form a catalytic diad (35, 36). The role of Asp^{99} was only resolved via NMR studies using a series of catalytic residue single/double mutants, which showed that Asp^{99} was directly hydrogen-bonded to the steroid (37).

Substrate Preference for Steroid trans-A/B Ring Fusion—AKR1C enzymes reduce 5α-DHT and 5β-DHT with similar catalytic efficiencies (23, 24). The preference of the AKR1D1 E120H mutant to reduce a 3-ketosteroid with an A/B *trans*-ring configuration over a *cis*-configuration by more than 10-fold was unexpected. This preference mainly results from the difference in substrate binding affinity, as reflected by a 10-fold difference in K_m values of 5α-DHT and 5β-DHT. The steroid binding channel of the E120H mutant has a cylindrical shape that packs the steroid tightly on three sides, where Tyr^{132} and Trp^{230} are parallel to the steroid plane, and Tyr^{26} is perpendicular to the steroid plane (Fig. 3*A*). This shape allows easy accommodation of 5α-DHT but not 5β-DHT that has a 90° bend at the A/B ring junction. By contrast, using AKR1C2 as an example, Tyr^{132} is replaced by a smaller residue, and the indole ring of Trp^{230} is placed almost perpendicular to its corresponding position in AKR1D1 (Fig. 3*C*). These changes forge the steroid binding channel into a curved shape that tolerates the *cis*-configuration better, resulting in a similar or even slightly favorable K_m for 5β-DHT over 5α-DHT in 3-ketosteroid reduction (Table 2).

Stereospecificity of 3-Ketosteroid/Hydroxysteroid Oxidoreduction—The majority of the AKR1C enzymes prefer the production of 3α-hydroxysteroids regardless of the steroid A/B-ring configuration. The AKR1D1 E120H mutant exhibits a different stereopreference. It acts as a 3β-HSD in the presence of 5α-DHT but produces a mixture of 3α- and 3β-hydroxysteroids in a 4:1 ratio when 5β-DHT is the substrate. Two mechanisms have been proposed to control the stereopreference of these HSDs, each through a unique motion of the steroid involving either swinging or flipping.

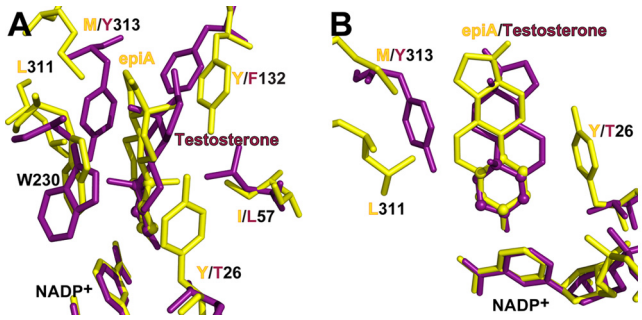

FIGURE 6. **Residues in the steroid binding channel in AKR1C9 (*purple*) and the AKR1D1 E120H mutant (*yellow*).** *A*, testosterone is tightly packed by Leu^{57} and Trp^{230} parallel to the steroid plane and Tyr^{313} perpendicular to the steroid plane. epiA is packed by Tyr^{132} and Trp^{230} parallel to the steroid plane and Tyr^{26} perpendicular to the steroid plane. The steroid A-rings are shown in *ball-and-stick representations*. *B*, a rotated view shows the residues that may be involved in the determination of stereospecificity. Residues are *numbered* as in AKR1D1.

The swinging mechanism was proposed based on docking simulations of 5α-DHT into AKR1C1 and AKR1C2, where the two enzymes show opposite stereospecificity for 5α-DHT reduction (23, 38). The docking models suggest that the steroid swings across the steroid binding pocket to present different faces for 4-pro-(*R*)-hydride transfer from the cofactor to ensure different stereochemical outcomes. This swinging mechanism is achieved by the size of the residue at position 57 (AKR1D1 numbering). The longer side chain of Leu^{57} in AKR1C1 pushes the steroid toward Trp^{230} so that the steroid α-face is presented to the cofactor to produce a 3β-hydroxysteroid, whereas the shorter side chain of Val^{57} in AKR1C2 ensures that the steroid β-face is presented to the cofactor to produce a 3α-hydoxysteroid. However, this mechanism cannot be applied to AKR1D1 because Ile^{57} is no longer in close proximity to the steroid and is unable to play a central role in steroid orientation. Also, this swinging mechanism may not be generalized to the other AKR1C enzymes because both AKR1C3 and AKR1C4 contain the Leu^{57} as in AKR1C1, yet they favor the production of the 3α-hydroxysteroid as seen in AKR1C2.

Our structures of the E120H mutant support a mechanism in which the faces of the steroid are flipped. The structures of the E120H·NADP$^+$·epiA and E120H·NADP$^+$·Δ^4-Adione complexes show that the steroid may present either its α- or β-face toward the cofactor by flipping 180° along its long molecular axis, using the stationary oxyanion site as the center of rotation (Figs. 3*A* and 4*A*). The flipping mechanism complies with the different stereopreference seen with the AKR1D1 E120H mutant and AKR1C9. The competitive inhibitor testosterone in AKR1C9 binds to the active site at almost the same position as epiA in the E120H mutant, except that the two steroids present opposite faces to the cofactor (*i.e.* the two steroids are flipped) (Fig. 6). Like the E120H mutant, AKR1C9 also packs testosterone on three sides, with Leu^{57} and Trp^{230} parallel to the steroid plane and Tyr^{313} perpendicular to the steroid plane, but Tyr^{313} in AKR1C9 resides on the opposite side of the steroid against Tyr^{26} in the E120H mutant. The tyrosine residues cause the steroid B-ring to be flipped away from them to avoid clashing, and, as a result, the α-face of the steroid is directed toward the cofactor for 3β-reduction in the E120H mutant, whereas the β-face of the steroid is directed toward the cofactor for 3α-reduction in AKR1C9.

Positional Specificity of Mutant—The E120H mutant exhibits residual activity at the 17- and 20-positions of the steroid. AKR1C enzymes possess this functional plasticity as well (Scheme 1) (8). The functional plasticity derives from the symmetric nature of the steroid molecule and the plasticity of the AKR1C active site. Among the ternary complex structures solved for the human AKR1C enzymes (12, 39–41), none of the structures depict steroids in a productive binding mode. Only in the AKR1C1·NADP$^+$·20α-OHP and AKR1C2·NADP$^+$·testosterone complexes do the steroids adopt orientations that correspond to observed positional preferences of the enzymes. The AKR1D1 E120H mutant catalyzes the 17β-hydroxysteroid oxidation of testosterone to yield Δ^4-Adione; however, the structure of the E120H·NADP$^+$·Δ^4-Adione complex also fails to display a productive binding mode (Fig. 4). Instead, a reverse binding orientation with the 3-ketone group tethered to the oxyanion site is observed. The preference for the 3-ketone over the 17β-hydroxyl group in the oxyanion site reflects the kinetic data, where the K_m values for the 3-ketosteroid reduction for 5α- and 5β-DHT are lower than the K_m values for the 17β-hydroxysteroid oxidation of the same steroids. In addition, the fact that the E120H mutant allows nonproductive binding of the substrate by reversing the A/D-ring orientation may be the cause of substrate inhibition observed with 5α-DHT, testosterone, and 20α-OHP in this mutant.

In conclusion, we have successfully engineered steroid 5β-reductase into a highly efficient 3β-HSD by a single glutamate-to-histidine mutation. The bulky histidine alters the shape of the active site, resulting in a shift of the relative position of the steroid to the cofactor, which changes the enzyme function. This E120H mutant elicits a change in stereospecificity of the HSD reaction by flipping the steroid, and it shows an unexpected preference for C19 steroids with a 5α-configuration over C19 steroids with a 5β-configuration due to the presence of a cylindrical binding channel. Engineered enzymes rarely exhibit adequate catalytic efficiency for a new activity with complete eradication of the native activity, but here we demonstrate an example of a perfect change of function achieved by a single point mutation.

Acknowledgments—We thank Dr. Julie A. Aaron for assistance in data collecting and processing and Dr. Yi Jin for helpful discussions. Part of this work was based upon research conducted at the Advanced Photon Source on the Northeastern Collaborative Access Team beamline 24_ID_C (supported by National Center for Research Resources, National Institutes of Health, Grant RR-15301). Use of the Advanced Photon Source, an Office of Science User Facility operated for the United States Department of Energy Office of Science by Argonne National Laboratory, was supported by the United States Department of Energy under Contract DE-AC02–06CH11357. Part of this work was based upon research conducted at beamline X29 of the National Synchrotron Light Source. Financial support comes principally from the Offices of Biological and Environmental Research and of Basic Energy Sciences of the United States Department of Energy and from National Center for Research Resources, National Institutes of Health, Grant P41RR012408.

REFERENCES

1. Kondo, K. H., Kai, M. H., Setoguchi, Y., Eggertsen, G., Sjöblom, P., Setoguchi, T., Okuda, K. I., and Björkhem, I. (1994) Cloning and expression of cDNA of human Δ^4-3-oxosteroid 5β-reductase and substrate specificity of the expressed enzyme. *Eur. J. Biochem.* **219,** 357–363
2. Russell, D. W., and Setchell, K. D. (1992) Bile acid biosynthesis. *Biochemistry* **31,** 4737–4749
3. Sheehan, P. M., Rice, G. E., Moses, E. K., and Brennecke, S. P. (2005) 5β-Dihydroprogesterone and steroid 5β-reductase decrease in association with human parturition at term. *Mol. Hum. Reprod.* **11,** 495–501
4. Granick, S., and Kappas, A. (1967) Steroid control of porphyrin and heme biosynthesis. A new biological function of steroid hormone metabolites. *Proc. Natl. Acad. Sci. U.S.A.* **57,** 1463–1467
5. Levere, R. D., Kappas, A., and Granick, S. (1967) Stimulation of hemoglobin synthesis in chick blastoderms by certain 5β-androstane and 5β-pregnane steroids. *Proc. Natl. Acad. Sci. U.S.A.* **58,** 985–990
6. Bertilsson, G., Heidrich, J., Svensson, K., Asman, M., Jendeberg, L., Sydow-Bäckman, M., Ohlsson, R., Postlind, H., Blomquist, P., and Berkenstam, A. (1998) Identification of a human nuclear receptor defines a new signaling pathway for CYP3A induction. *Proc. Natl. Acad. Sci. U.S.A.* **95,** 12208–12213
7. Moore, L. B., Parks, D. J., Jones, S. A., Bledsoe, R. K., Consler, T. G., Stimmel, J. B., Goodwin, B., Liddle, C., Blanchard, S. G., Willson, T. M., Collins, J. L., and Kliewer, S. A. (2000) Orphan nuclear receptors constitutive androstane receptor and pregnane X receptor share xenobiotic and steroid ligands. *J. Biol. Chem.* **275,** 15122–15127
8. Penning, T. M., Burczynski, M. E., Jez, J. M., Hung, C. F., Lin, H. K., Ma, H., Moore, M., Palackal, N., and Ratnam, K. (2000) Human 3α-hydroxysteroid dehydrogenase isoforms (AKR1C1–AKR1C4) of the aldo-keto reductase superfamily. Functional plasticity and tissue distribution reveals roles in the inactivation and formation of male and female sex hormones. *Biochem. J.* **351,** 67–77
9. Penning, T. M., and Drury, J. E. (2007) Human aldo-keto reductases. Function, gene regulation, and single nucleotide polymorphisms. *Arch. Biochem. Biophys.* **464,** 241–250
10. Di Costanzo, L., Drury, J. E., Penning, T. M., and Christianson, D. W. (2008) Crystal structure of human liver Δ^4-3-ketosteroid 5β-reductase (AKR1D1) and implications for substrate binding and catalysis. *J. Biol. Chem.* **283,** 16830–16839
11. Bennett, M. J., Albert, R. H., Jez, J. M., Ma, H., Penning, T. M., and Lewis, M. (1997) Steroid recognition and regulation of hormone action. Crystal structure of testosterone and $NADP^+$ bound to 3α-hydroxysteroid/dihydrodiol dehydrogenase. *Structure* **5,** 799–812
12. Jin, Y., Stayrook, S. E., Albert, R. H., Palackal, N. T., Penning, T. M., and Lewis, M. (2001) Crystal structure of human type III 3α-hydroxysteroid dehydrogenase/bile acid-binding protein complexed with $NADP^+$ and ursodeoxycholate. *Biochemistry* **40,** 10161–10168
13. Berséus, O., and Björkhem, L. (1967) Enzymatic conversion of a Δ^4-3-ketosteroid into a 3α-hydroxy-5β steroid. Mechanism and stereochemistry of hydrogen transfer from NADPH. Bile acids and steroids 190. *Eur. J. Biochem.* **2,** 503–507
14. Schlegel, B. P., Jez, J. M., and Penning, T. M. (1998) Mutagenesis of 3α-hydroxysteroid dehydrogenase reveals a "push-pull" mechanism for proton transfer in aldo-keto reductases. *Biochemistry* **37,** 3538–3548
15. Jez, J. M., Bennett, M. J., Schlegel, B. P., Lewis, M., and Penning, T. M. (1997) Comparative anatomy of the aldo-keto reductase superfamily. *Biochem. J.* **326,** 625–636
16. Norymberski, J. K., and Woods, G. F. (1955) Partial reduction of steroid hormones and related substances. *J. Chem. Soc.* **76,** 3426–3430
17. March, J. (1984) *Advanced Organic Chemistry: Reactions, Mechanism and Structure*, pp. 694–695, John Wiley & Sons, Inc., New York
18. Otwinowski, Z., and Minor, W. (1997) Processing of X-ray diffraction data collected in oscillation mode. *Methods Enzymol.* **276,** 307–326
19. McCoy, A. J., Grosse-Kunstleve, R. W., Adams, P. D., Winn, M. D., Storoni, L. C., and Read, R. J. (2007) Phaser crystallographic software. *J. Appl. Crystallogr.* **40,** 658–674
20. Brunger, A. T., Adams, P. D., Clore, G. M., Delano, W. L., Gros, P., Grosse-Kunstleve, R. W., Jiang, J. S., Kuszewski, J., Nilges, N., Pannu, N. S., Read, R. J., Rice, L. M., Simonson, T., and Warren, G. L. (1998) Crystallography & NMR system. A new software suite for macromolecular structure determination. *Acta Crystallogr. D* **54,** 905–921
21. Adams, P. D., Afonine, P. V., Bunkóczi, G., Chen, V. B., Davis, I. W., Echols, N., Headd, J. J., Hung, L. W., Kapral, G. J., Grosse-Kunstleve, R. W., McCoy, A. J., Moriarty, N. W., Oeffner, R., Read, R. J., Richardson, D. C., Richardson, J. S., Terwilliger, T. C., and Zwart, P. H. (2010) PHENIX. A comprehensive Python-based system for macromolecular structure solution. *Acta Crystallogr. D* **66,** 213–221
22. Emsley, P., and Cowtan, K. (2004) Coot. Model-building tools for molecular graphics. *Acta Crystallogr. D* **60,** 2126–2132
23. Jin, Y., Duan, L., Lee, S. H., Kloosterboer, H. J., Blair, I. A., and Penning, T. M. (2009) Human cytosolic hydroxysteroid dehydrogenases of the aldo-ketoreductase superfamily catalyze reduction of conjugated steroids. Implications for phase I and phase II steroid hormone metabolism. *J. Biol. Chem.* **284,** 10013–10022
24. Jin, Y., Mesaros, A. C., Blair, I. A., and Penning, T. M. (2011) Stereospecific reduction of 5β-reduced steroids by human ketosteroid reductases of the AKR (aldo-keto reductase) superfamily. Role of AKR1C1-AKR1C4 in the metabolism of testosterone and progesterone via the 5β-reductase pathway. *Biochem. J.* **437,** 53–61
25. Faucher, F., Cantin, L., Luu-The, V., Labrie, F., and Breton, R. (2008) The crystal structure of human Δ^4-3-ketosteroid 5β-reductase defines the functional role of the residues of the catalytic tetrad in the steroid double bond reduction mechanism. *Biochemistry* **47,** 8261–8270
26. Chen, M., Drury, J. E., and Penning, T. M. (2011) Substrate specificity and inhibitor analyses of human steroid 5β-reductase (AKR1D1). *Steroids* **76,** 484–490
27. Di Costanzo, L., Drury, J. E., Christianson, D. W., and Penning, T. M. (2009) Structure and catalytic mechanism of human steroid 5β-reductase (AKR1D1). *Mol. Cell. Endocrinol.* **301,** 191–198
28. Steckelbroeck, S., Jin, Y., Gopishetty, S., Oyesanmi, B., and Penning, T. M. (2004) Human cytosolic 3α-hydroxysteroid dehydrogenases of the aldo-keto reductase superfamily display significant 3β-hydroxysteroid dehydrogenase activity. Implications for steroid hormone metabolism and action. *J. Biol. Chem.* **279,** 10784–10795
29. Simard, J., Ricketts, M. L., Gingras, S., Soucy, P., Feltus, F. A., and Melner, M. H. (2005) Molecular biology of the 3β-hydroxysteroid dehydrogenase/Δ^5-Δ^4-isomerase gene family. *Endocr. Rev.* **26,** 525–582
30. Jez, J. M., and Penning, T. M. (1998) Engineering steroid 5β-reductase activity into rat liver 3α-hydroxysteroid dehydrogenase. *Biochemistry* **37,** 9695–9703
31. Okuda, A., and Okuda, K. (1984) Purification and characterization of Δ^4-3-ketosteroid 5β-reductase. *J. Biol. Chem.* **259,** 7519–7524
32. Thorn, A., Egerer-Sieber, C., Jäger, C. M., Herl, V., Müller-Uri, F., Kreis, W., and Muller, Y. A. (2008) The crystal structure of progesterone 5β-reductase from *Digitalis lanata* defines a novel class of short chain dehydrogenases/reductases. *J. Biol. Chem.* **283,** 17260–17269
33. Kim, S. W., Cha, S. S., Cho, H. S., Kim, J. S., Ha, N. C., Cho, M. J., Joo, S., Kim, K. K., Choi, K. Y., and Oh, B. H. (1997) High-resolution crystal structures of Δ^5-3-ketosteroid isomerase with and without a reaction intermediate analogue. *Biochemistry* **36,** 14030–14036
34. Wu, Z. R., Ebrahimian, S., Zawrotny, M. E., Thornburg, L. D., Perez-Alvarado, G. C., Brothers, P., Pollack, R. M., and Summers, M. F. (1997) Solution structure of 3-oxo-Δ^5-steroid isomerase. *Science* **276,** 415–418
35. Zhao, Q., Abeygunawardana, C., Gittis, A. G., and Mildvan, A. S. (1997) Hydrogen bonding at the active site of Δ^5-3-ketosteroid isomerase. *Biochemistry* **36,** 14616–14626
36. Massiah, M. A., Abeygunawardana, C., Gittis, A. G., and Mildvan, A. S. (1998) Solution structure of Δ^5-3-ketosteroid isomerase complexed with the steroid 19-nortestosterone hemisuccinate. *Biochemistry* **37,** 14701–14712
37. Cho, H. S., Ha, N. C., Choi, G., Kim, H. J., Lee, D., Oh, K. S., Kim, K. S., Lee, W., Choi, K. Y., and Oh, B. H. (1999) Crystal structure of Δ^5-3-ketosteroid isomerase from *Pseudomonas testosteroni* in complex with equilenin settles the correct hydrogen bonding scheme for transition state stabilization. *J. Biol. Chem.* **274,** 32863–32868

38. Jin, Y., and Penning, T. M. (2006) Molecular docking simulations of steroid substrates into human cytosolic hydroxysteroid dehydrogenases (AKR1C1 and AKR1C2). Insights into positional and stereochemical preferences. *Steroids* **71,** 380–391
39. Couture, J. F., Legrand, P., Cantin, L., Luu-The, V., Labrie, F., and Breton, R. (2003) Human 20α-hydroxysteroid dehydrogenase. Crystallographic and site-directed mutagenesis studies lead to the identification of an alternative binding site for C21-steroids. *J. Mol. Biol.* **331,** 593–604
40. Qiu, W., Zhou, M., Labrie, F., and Lin, S. X. (2004) Crystal structures of the multispecific 17β-hydroxysteroid dehydrogenase type 5. Critical androgen regulation in human peripheral tissues. *Mol. Endocrinol.* **18,** 1798–1807
41. Nahoum, V., Gangloff, A., Legrand, P., Zhu, D. W., Cantin, L., Zhorov, B. S., Luu-The, V., Labrie, F., Breton, R., and Lin, S. X. (2001) Structure of the human 3α-hydroxysteroid dehydrogenase type 3 in complex with testosterone and NADP at 1.25 Å resolution. *J. Biol. Chem.* **276,** 42091–42098
42. Laskowski, R. A., MacArthur, M. W., Moss, D. S., and Thornton, J. M. (1993) PROCHECK. A program to check the stereochemical quality of protein structures. *J. Appl. Crystallogr.* **26,** 283–291